

# Triarylamine-Substituted Imidazole- and Quinoxaline-Fused Push–Pull Porphyrins for Dye-Sensitized Solar Cells

Hironobu Hayashi,<sup>[a]</sup> Abeda Sultana Touchy,<sup>[b]</sup> Yuriko Kinjo,<sup>[a]</sup> Kei Kurotobi,<sup>[b]</sup> Yuuki Toude,<sup>[a]</sup> Seigo Ito,<sup>[c]</sup> Hanna Saarenpää,<sup>[d]</sup> Nikolai V. Tkachenko,<sup>[d]</sup> Helge Lemmetyinen,<sup>[d]</sup> and Hiroshi Imahori<sup>\*[a, b]</sup>

We have prepared a push–pull porphyrin with an electron-donating triarylamo group at the  $\beta,\beta'$ -edge through a fused imidazole group and an electron-withdrawing carboxyquinoxalino anchoring group at the opposite  $\beta,\beta'$ -edge (ZnPQI) and evaluated the effects of the push–pull structure of ZnPQI on optical, electrochemical, and photovoltaic properties. ZnPQI showed red-shifted Soret and Q bands relative to a reference porphyrin with only an electron-withdrawing group (ZnPQ), thus demonstrating the improved light-harvesting property of ZnPQI. The optical HOMO–LUMO gap was consistent with that estimated by DFT calculations. The ZnPQI-sensitized solar cell

exhibited a relatively high power conversion efficiency ( $\eta$ ) of 6.8%, which is larger than that of the ZnPQ-sensitized solar cell ( $\eta=6.3\%$ ) under optimized conditions. The short-circuit current and fill factor of the ZnPQI-sensitized solar cell are larger than those of the ZnPQ-sensitized solar cell, whereas the open circuit potential of the ZnPQI-sensitized cell is smaller than that of the ZnPQ-sensitized cell, leading to an overall improved cell performance of ZnPQI. Such fundamental information provides a new tool for the rational molecular design of highly efficient dye-sensitized solar cells based on push–pull porphyrins.

## Introduction

We have been reliant on fossil fuels to produce an enormous amount of energy. However, there is a limit of fossil-fuel reserves, and they surely will be exhausted sooner or later. Therefore, there is a need to develop sustainable and clean-energy-producing systems.<sup>[1]</sup> In this regard, solar cells have attracted much attention due to their direct conversion of solar energy into electricity. In particular, a great deal of attention has been devoted to dye-sensitized solar cells (DSSCs) made from mesoporous  $\text{TiO}_2$  electrodes owing to the possibility of

low-cost production and high power conversion efficiency ( $\eta$ ).<sup>[2]</sup>

Until recently, ruthenium(II) bipyridyl complexes have proven to be the most efficient  $\text{TiO}_2$  sensitizers.<sup>[3]</sup> However, in view of the high cost and scarcity of ruthenium, organic dyes without metals or inexpensive metal complexes are desirable for highly efficient DSSCs.<sup>[4,5]</sup> To attain highly efficient solar energy conversion, such organic dyes should fulfill the following requirements: 1) broad light-absorption capability that allows us to collect solar light efficiently in visible and near-infrared regions, 2) fast electron injection from the excited dyes to a conduction band (CB) of the  $\text{TiO}_2$  electrode, 3) slow charge recombination between the injected electrons and resulting dye cations or  $\text{I}_3^-$  in the electrolyte. So far, organic dyes composed of  $\pi$ -conjugative molecules, such as coumarin,<sup>[6]</sup> indoline,<sup>[7]</sup> polyene,<sup>[8]</sup> thiophene,<sup>[9]</sup> cyanine,<sup>[10]</sup> hemicyanine,<sup>[11]</sup> squaraine,<sup>[12]</sup> phthalocyanine,<sup>[13]</sup> perylenes,<sup>[14]</sup> and tetrathiafulvalene<sup>[15]</sup> derivatives have been explored as potential sensitizers for DSSCs.

Porphyrins are among the most widely studied sensitizers for DSSCs because of their strong Soret (400–450 nm) and moderate Q bands (550–600 nm).<sup>[16–23]</sup> More importantly, their optical, electrochemical, and photophysical properties can be modulated by peripheral substitutions and inner metal complexations. Nevertheless, until recently porphyrins as sensitizers typically have shown poor cell performances relative to ruthenium polypyridyl complexes. The major cause resulted from insufficient light-harvesting abilities of typical porphyrins in optimized cells, especially at around 500 nm and at wavelengths beyond 600 nm.<sup>[5a, 19d]</sup> To overcome this drawback, the pertur-

[a] Dr. H. Hayashi, Y. Kinjo, Y. Toude, Prof. H. Imahori  
Department of Molecular Engineering  
Graduate School of Engineering  
Kyoto University  
Nishikyo-ku, Kyoto 615-8510 (Japan)

[b] Dr. A. S. Touchy, Prof. K. Kurotobi, Prof. H. Imahori  
Institute for Integrated Cell-Material Sciences (WPI-iCeMS)  
Kyoto University  
Nishikyo-ku, Kyoto 615-8510 (Japan)  
Fax: (+81) 75-383-2571  
E-mail: imahori@scl.kyoto-u.ac.jp

[c] Prof. S. Ito  
Department of Electrical Engineering and Computer Sciences  
Graduate School of Engineering  
University of Hyogo  
2167 Shosha, Himeji, Hyogo 671-2280 (Japan)

[d] H. Saarenpää, Prof. N. V. Tkachenko, Prof. H. Lemmetyinen  
Department of Chemistry and Bioengineering  
Tampere University of Technology  
P.O. Box 541, FIN-33101 Tampere (Finland)

 Supporting Information for this article is available on the WWW under  
<http://dx.doi.org/10.1002/cssc.201200869>.

bation of the porphyrin  $\pi$  system is an effective methodology to tailor the optical, photophysical, and electrochemical properties. For instance, a push–pull porphyrin with an electron-donating diarylaminogroup at the *meso* position and an electron-withdrawing carboxyphenylethynyl anchoring group at the opposite *meso* position led to a remarkably improved  $\eta$  value of up to 12.3%, which was achieved by co-sensitization with an organic dye under standard air mass (AM) 1.5 conditions.<sup>[23g,j]</sup>

We have also proposed that the unsymmetrical  $\pi$  elongation of porphyrins is a promising strategy to improve light-harvesting properties.<sup>[5a,20]</sup> Especially quinoxalino[2,3-*b*]porphyrin acid (ZnPQ, Figure 1) showed broadened, red-shifted, and amplified

introduction of the electron-donating triarylarnino group as a result of enhanced charge-transfer (CT) character,<sup>[4–15]</sup> which would have a significant impact on the photovoltaic properties. Overall, we can evaluate the substituent effects of the triarylarnino group through the fused imidazole moiety as an electron-donating group on the optical, electrochemical, and photovoltaic properties of the porphyrins.

## Results and Discussion

### Synthesis and characterization

The key features of the synthetic route to ZnPQI involve the stepwise asymmetrical functionalization of symmetrical *meso*-tetraarylporphyrin to build up the push–pull molecular structure of ZnPQI (Scheme 1). Therefore, ZnPQI was designed to possess the fused imidazole group at one side of the porphyrin ring and the fused quinoxaline group at the opposite side. The starting compounds 2-(4-bromophenyl)-5,5-dimethyl-1,3-dioxane (**1**) and bis(4-hexylphenyl)amine (**2**) were prepared following literature procedures.<sup>[24,25]</sup> The coupling of **1** and **2** yielded the protected triarylamine **3**. Formyl triarylamine (**4**) was obtained by acidic hydrolysis of **3**. Porphyrin dione **7** was prepared by acetoxylation of *meso*-tetraarylporphyrin **5** and subsequent oxidation of **6**, which was employed for the next oxidation reaction without isolation, according to established methods.<sup>[26]</sup> Subsequent acetoxylation of **7** followed by oxidation of **8** yielded porphyrin tetraone **9**.<sup>[27]</sup> The coupling of **9** with **4** under mild acidic conditions led to a triarylamine-substituted imidazole-fused porphyrin dione (**10**). The condensation of **10** with methyl diaminobenzoate in pyridine afforded the desired triarylamine-substituted imidazole and quinoxaline fused porphyrin (**11**). Finally, treatment of **11** with zinc acetate followed by hydrolysis under basic conditions yielded ZnPQI. Initially, we attempted to synthesize **11** through a different synthetic route: the synthesis of quinoxaline-fused porphyrin dione from quinoxaline fused porphyrin, as in our previous report,<sup>[20h]</sup> followed by condensation with **4** to yield **11**. Unfortunately, the quinoxaline fused porphyrin dione did not react with **4**, resulting in decomposition of the porphyrin. Structures of all new compounds were verified by performing  $^1\text{H}$  NMR, IR, and high resolution MS (HRMS) analyses (see the Supporting Information).

$^1\text{H}$  NMR spectra of ZnPQI showed a broad singlet resonance at 8.6 ppm, which is assigned to the imidazole NH group. The broad signal suggests that imidazole tautomerization occurs on the  $^1\text{H}$  NMR timescale at room temperature as seen in previous reports.<sup>[27]</sup> Considering that regioisomers of dyes have an impact on device performance<sup>[28]</sup> and ZnPQI involves the imidazole moiety and a carboxylic acid group at the quinoxaline ring, this slow tautomerization of the imidazole NH group may affect device performance.

### Spectroscopic and electrochemical studies

Figure 2 displays UV/Vis absorption spectra of ZnPQI and ZnPQ<sup>[20g,h]</sup> in dichloromethane. Peak positions and molar ab-

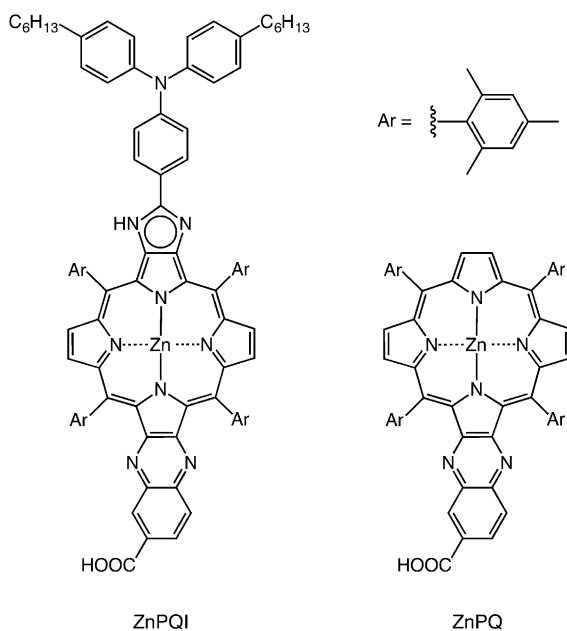
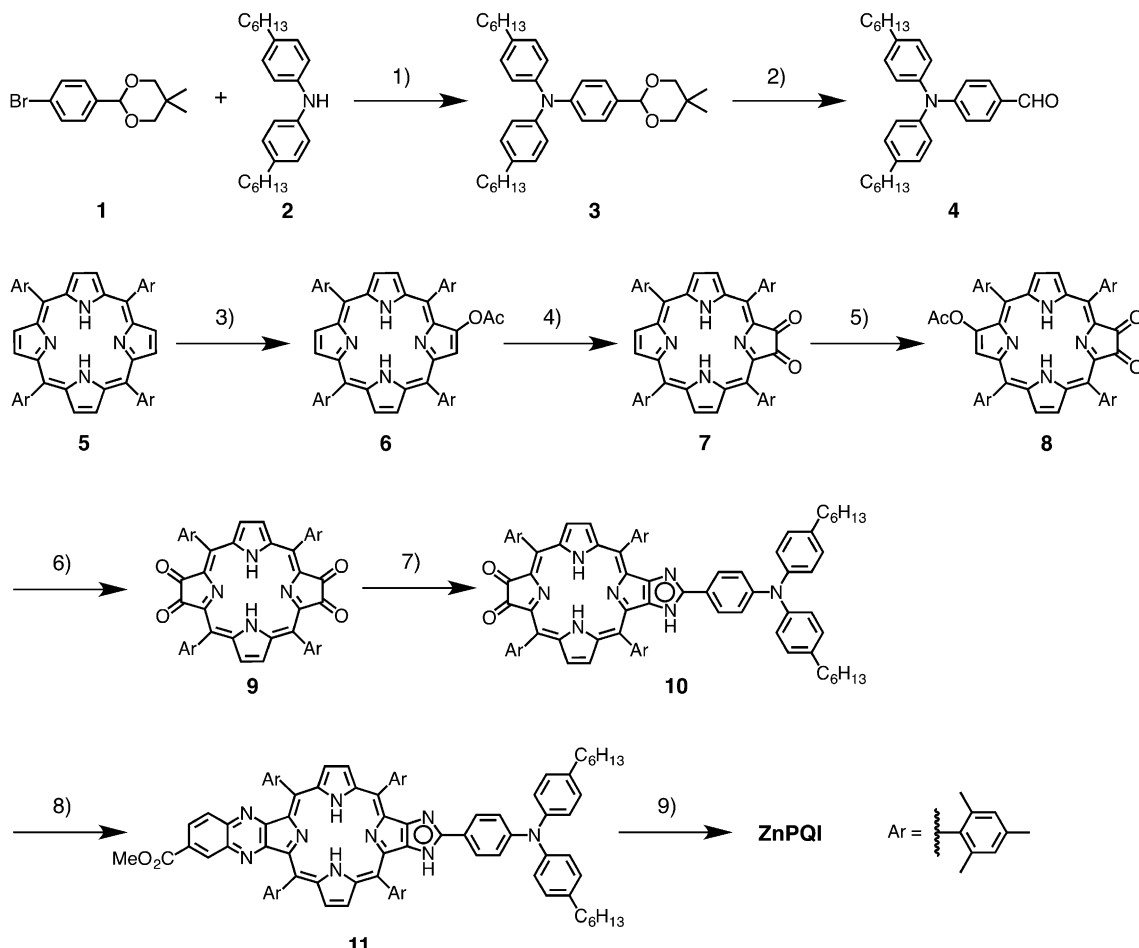


Figure 1. Molecular structures used in this study.

light-absorption properties relative to those of the corresponding porphyrin reference, resulting in  $\eta$  values of 6.3%.<sup>[5a,20g,h]</sup> Therefore, quinoxaline-fused porphyrins are highly attractive as excellent sensitizers for DSSCs. On the other hand, introduction of both electron-donating and electron-withdrawing substituents, including an anchoring group to the core of the  $\pi$  system, is also appealing for the modulation of the light-harvesting properties of sensitizers, as demonstrated for other sensitizers in DSSCs.<sup>[4–15]</sup> Considering that the fused quinoxaline group of ZnPQ possesses an electron-withdrawing character, the additional introduction of an electron-donating group into the ZnPQ core is expected to enhance the light-harvesting properties of the sensitizer.

Herein, we report the synthesis and the optical, electrochemical, and photovoltaic properties of a push–pull porphyrin with an electron-withdrawing carboxyquinoxalino anchoring group at the  $\beta,\beta'$ -edge and an electron-donating triarylarnino group at the opposite  $\beta,\beta'$ -edge through a fused imidazole moiety (ZnPQI, Figure 1). We expected that the absorption of the porphyrin would be broadened and red-shifted by the in-



**Scheme 1.** Synthesis of ZnPQI: 1)  $t\text{Bu}_3\text{PPhBF}_4$ ,  $[\text{Pd}_2(\text{dba})_3]$  ( $\text{dba} = \text{dibenzylideneacetone}$ ),  $\text{NaOtBu}$ , toluene, 26 h, 56%; 2) trifluoroacetic acid, aq.  $\text{H}_2\text{SO}_4$  (10%), 2.5 h, 96%; 3) silver acetate, iodine, dichloromethane, 4 h; 4) a)  $\text{K}_2\text{CO}_3$ , methanol, dichloromethane, 8 h; b) Dess–Martin–Periodinane (DMP), dichloromethane, 4 h, 15% (two steps); 5) silver acetate, iodine, dichloromethane, 4 h; 6) a)  $\text{K}_2\text{CO}_3$ , methanol, dichloromethane, 8 h; b) DMP, dichloromethane, 4 h, 14% (two steps); 7) 4,  $\text{NH}_4\text{OAc}$ , chloroform/acetic acid (9:1), reflux, 10 h; 8) methyl 3,4-diaminobenzoate, pyridine, 110 °C, 20 h, 20% (two steps). 9) a)  $\text{Zn}(\text{OAc})_2$ , methanol, dichloromethane, 8 h; b) aq. KOH, THF/EtOH (1:1), reflux, 4 h; c) aq.  $\text{NH}_4\text{Cl}$ , dichloromethane, 8 h, 96%.

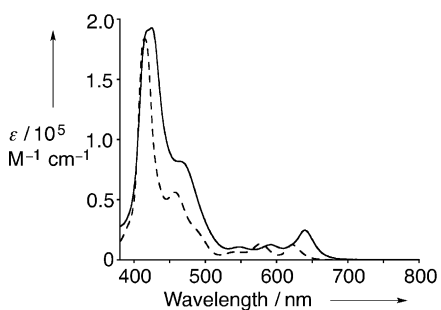


**Figure 2.** UV/Vis absorption spectra of ZnPQI (solid line) and ZnPQ<sup>[20g,h]</sup> (dashed line) measured in dichloromethane.

sorption coefficients ( $\epsilon$ ) of Soret and Q bands are listed in Table 1. The Soret band of ZnPQI is split into two peaks and becomes broader, and is shifted toward longer wavelengths relative to that of ZnPQ. In addition, the Q bands are also red-shifted relative to ZnPQ. The absorption properties of ZnPQI are beneficial for harnessing solar energy in the visible region.

The steady-state fluorescence spectrum of ZnPQI was measured in dichloromethane by exciting at the strongest peak positions of the Soret bands (see the Supporting Information, Figure S1). The wavelengths for emission maxima are listed in Table 1. In accordance with the trend of the absorption maximum on the longest wavelength side, the emission maximum of ZnPQI is red-shifted relative to that of ZnPQ<sup>[20g,h]</sup>. From the intersection of normalized absorption and emission spectra, the zero-zero excitation energy ( $E_{0-0}$ ) is determined to be 1.92 eV for ZnPQI, which is smaller than that of ZnPQ<sup>[20g,h]</sup> (Table 1). The fluorescence lifetime ( $\tau$ ) of ZnPQI was obtained in dichloromethane by a time-correlated single-photon counting technique.<sup>[29]</sup> The excitation wavelength was 405 nm and fluorescence was monitored at the strongest emission maximum for ZnPQI. The decay curve of the fluorescence intensity was single exponential and was fitted to give  $\tau = (1.25 \pm 0.01)$  ns for ZnPQI, which is significantly longer than  $\tau = (0.99 \pm 0.01)$  ns for ZnPQ<sup>[20g,h]</sup>. Because electron-injection processes from the excited dyes to a conduction band (CB) of TiO<sub>2</sub> take place on a time scale of 0.1–100 ps,<sup>[30,31]</sup> the relatively slow

Table 1. Optical and electrochemical data for porphyrins and driving forces for electron transfer processes on TiO <sub>2</sub> .									
	$\lambda_{\text{abs}}^{[a]}$ [nm]	$\varepsilon$ [10 <sup>3</sup> M <sup>-1</sup> cm <sup>-1</sup> ]	$\lambda_{\text{em}}^{[b]}$ [nm]	$E_{\text{ox}}^{[c]}$ [V]	$E_{\text{red}}^{[c]}$ [V]	$E_{0-0}$ [eV]	$E_{\text{ox}}^{*^{[d]}}$ [V]	$\Delta G_{\text{inj}}^{[e]}$ [eV]	$\Delta G_{\text{reg}}^{[f]}$ [eV]
ZnPQI	416	188	660	0.92	-1.11	1.92	-1.00	-0.50	-0.42
	424	193							
	470	122							
	548	16.8							
	594	19.2							
	641	36.9							
ZnPQ <sup>[g]</sup>	415	184	645	0.98	-1.13	1.98	-1.00	-0.50	-0.48
	458	56.2							
	578	13.6							
	622	12.6							

[a] Wavelengths for Soret and Q-band maxima in CH<sub>2</sub>Cl<sub>2</sub>. [b] Wavelengths for emission maxima in CH<sub>2</sub>Cl<sub>2</sub> by exciting at Soret wavelength. [c] First oxidation and reduction potentials (versus NHE). [d] Excited-state oxidation potentials approximated from  $E_{\text{ox}}$  and  $E_{0-0}$  (versus NHE). [e] Driving forces for electron injection from the porphyrin singlet excited state ( $E_{\text{ox}}^*$ ) to the CB of TiO<sub>2</sub> (-0.5 V versus NHE). [f] Driving forces for the regeneration of porphyrin radical cation ( $E_{\text{ox}}$ ) by the I<sup>-</sup>/I<sub>3</sub><sup>-</sup> redox couple (+0.5 V versus NHE). [g] From Ref. [20g].

fluorescence decay of ZnPQI may have little influence on electron-injection efficiency ( $\phi_{\text{inj}}$ ).

To determine the first oxidation potential ( $E_{\text{ox}}$ ) and the first reduction potential ( $E_{\text{red}}$ ) of ZnPQI in solution, differential pulse voltammetry (DPV) measurements were performed in dichloromethane containing Bu<sub>4</sub>NPF<sub>6</sub> (0.1 M) as a supporting electrolyte (Table 1 and also see the Supporting Information, Figure S2). The  $E_{\text{ox}}$  value of ZnPQI was 0.92 V versus the normal hydrogen electrode (NHE) and is shifted significantly to a negative direction relative to ZnPQ (0.98 V versus NHE),<sup>[20g]</sup> but the  $E_{\text{red}}$  value of ZnPQI (-1.11 V versus NHE) is almost similar to that of ZnPQ (-1.13 V versus NHE).<sup>[20g]</sup> This implies that the introduction of the electron-donating group, including the triarylarnino and fused imidazole moieties, affects the HOMO of the porphyrin rather than the LUMO. This trend leads to a decrease in the electrochemical HOMO-LUMO gaps. However, the difference in HOMO levels of ZnPQI and ZnPQ is moderate, despite the presence of the triphenylamino and fused imidazole moieties in ZnPQI. Fusion of imidazole to  $\beta$ -positions of a porphyrin ring does not contribute to the extension of the porphyrin  $\pi$  system significantly.<sup>[27]</sup> Although DFT calculations predict the coplanarity between the porphyrin core and the phenylene spacer attached to the diarylarnino moiety, the energy barrier around the phenylene spacer against the fused imidazole moiety would be small, resulting in an unexpectedly subdued effect of  $\pi$  conjugation in ZnPQI (vide infra). The electrochemical HOMO-LUMO gap of ZnPQI is determined to be 2.03 eV, which is considerably smaller than that of ZnPQ (2.11 eV).<sup>[20g]</sup> The trend largely agrees with that of the optical HOMO-LUMO gaps (vide supra).

From spectroscopic and electrochemical measurements, driving forces for electron injection from the porphyrin excited singlet state to the CB of the TiO<sub>2</sub> (-0.50 V versus NHE;  $\Delta G_{\text{inj}}$ ) and the regeneration of the porphyrin radical cation by the I<sup>-</sup>/I<sub>3</sub><sup>-</sup> redox couple (-0.42 V versus NHE;  $\Delta G_{\text{reg}}$ ) for the ZnPQI-sensitized solar cell are determined (Table 1).<sup>[20]</sup> Both processes are thermodynamically feasible and sufficient for efficient electron transfer (< -0.3 eV; vide infra).

## DFT calculations

DFT calculations were employed to gain insight into the equilibrium geometry and electronic structures for the frontier orbitals of the porphyrins. The calculated structures do not show negative frequencies, implying that the optimized geometry is in the global energy minimum.<sup>[32]</sup> Notably, ZnPQI possesses a conjugated planar linkage extending from the quinoxaline moiety to the phenylene ring attached to the imidazole moiety,<sup>[27b]</sup> whereas the 2,4,6-trimethylphenyl groups are almost perpendicular to the

porphyrin core to avoid the steric congestion around the meso-positions<sup>[20d]</sup> (see the Supporting Information, Figure S3). However, on the basis of cyclic voltammetry measurements, there is a possibility that ZnPQI possesses the orthogonal disposition of the phenylene spacer against the fused imidazole moiety and therefore the low conjugation between the electrons of the N atom and the aromatic cloud of the porphyrin, as seen in triarylarnino moieties that are introduced at the meso-position of porphyrins for DSSCs.<sup>[33]</sup> Rotation of the phenylene spacer against the imidazole moiety would have little influence on an energy level of the optimized structure by DFT calculations.

Porphyrins with  $D_{4h}$  symmetry generally reveal two energetically degenerate LUMOs (LUMO+1, LUMO) and two nearly degenerate HOMOs (HOMO, HOMO-1).<sup>[20]</sup> The degenerate energy levels of LUMO and LUMO+1 are split in both ZnPQI and ZnPQ<sup>[20g]</sup> (Table 2). Although the degenerate energy levels of HOMO and HOMO-1 are split significantly in ZnPQI, the near degeneracy of HOMO and HOMO-1 is retained for ZnPQ. The theoretical HOMO-LUMO gaps of these porphyrins are as follows: ZnPQ (2.69 eV)<sup>[20g]</sup> > ZnPQI (2.26 eV). This trend is in

Table 2. Molecular orbital energy levels for porphyrins.<sup>[a]</sup>

Orbital	Energy level [ev] ZnPQI	Energy level [ev] ZnPQ <sup>[b]</sup>
LUMO+1	-2.08	-2.23
LUMO	-2.55 (-3.33) <sup>[c]</sup>	-2.56 (-3.31) <sup>[c]</sup>
HOMO	-4.81 (-5.36) <sup>[c]</sup>	-5.25 (-5.42) <sup>[c]</sup>
HOMO-1	-5.05	-5.28

[a] Some sets of molecular orbital energy levels for porphyrins were estimated by DFT calculations with B3LYP/6-31G(d). The energies in eV are quoted with respect to the vacuum (1 Hartree = 27.2116 eV). [b] From Ref. [20g]. [c] The energy levels of HOMO and LUMO were determined electrochemically, given that the absolute energy level of NHE is -4.44 eV under vacuum.

good agreement with those of the optical and electrochemical HOMO–LUMO gaps (vide infra).

Figure 3 illustrates the electron-density distributions of ZnPQI and ZnPQ in their respective HOMOs and LUMOs. The electron-density distribution of LUMOs around an anchoring

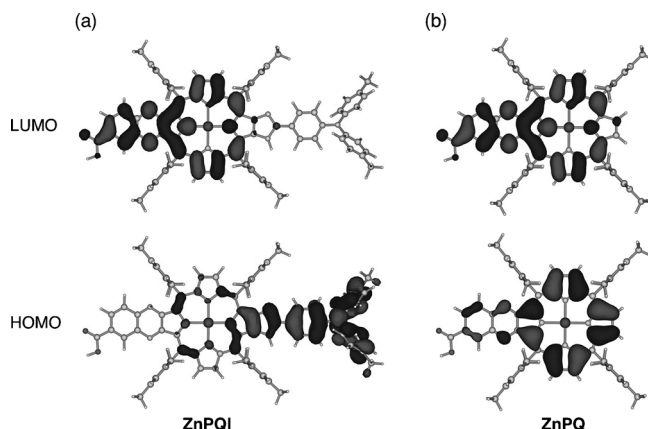


**Figure 3.** Sets of molecular orbital diagrams for (a) ZnPQI and (b) ZnPQ<sup>[20d]</sup> obtained by DFT calculations with B3LYP/6-31G(d).

group influences the electronic coupling between the excited adsorbed dye and the 3d orbital of TiO<sub>2</sub>.<sup>[34]</sup> The quinoxaline group, including the anchoring moiety, possesses slightly smaller electron densities in the LUMO of ZnPQI (29.8%) relative to those in the LUMO of ZnPQ (32.8%). Accordingly, we can anticipate the efficient  $\phi_{inj}$  value of ZnPQI from the porphyrin excited singlet state to the CB of TiO<sub>2</sub>, as in the case of ZnPQ<sup>[20g,h]</sup> (vide infra). On the other hand, the electron density of the HOMO is mainly distributed in the triarylamine-substituted imidazole moiety, which is at the opposite side of the fused quinoxaline moiety. These results are consistent with the expected push–pull electronic structure of ZnPQI.

### Porphyrin adsorption on TiO<sub>2</sub>

The TiO<sub>2</sub> electrodes were immersed into solutions of ZnPQI in ethanol (0.2 mM) to yield the porphyrin-stained TiO<sub>2</sub> electrodes. Total amounts of the porphyrins adsorbed on TiO<sub>2</sub> films were determined by measuring the difference in absorbance of the TiO<sub>2</sub> films without the scattering layer before and after immersion of the TiO<sub>2</sub> film into the porphyrin solution in ethanol. After immersion, ZnPQI in EtOH reached almost saturated surface coverage ( $\Gamma$ ) on the TiO<sub>2</sub> films in 4 h (Figure 4). The trend is similar to our previous report on the  $\Gamma$  value of ZnPQ on TiO<sub>2</sub> as a function of immersion time,<sup>[20d,f,g]</sup> but the adsorption speed of ZnPQI is slower than that of ZnPQ, which agrees with the small electron density of the quinoxaline group including the anchoring moiety in the LUMO of ZnPQI relative to ZnPQ.<sup>[20]</sup> The saturated  $\Gamma$  value of ZnPQI on the TiO<sub>2</sub> film is determined to be about  $1.0 \times 10^{-10} \text{ mol cm}^{-2}$ , which is comparable to that of ZnPQ ( $1.1 \times 10^{-10} \text{ mol cm}^{-2}$ ). Assuming that the porphyrin monolayer is densely packed and vertically orientated to the TiO<sub>2</sub> surface, the  $\Gamma$  value of ZnPQI is calculated to be

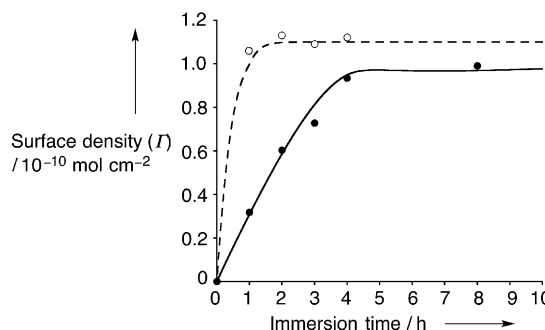


**Figure 4.** Plots of porphyrin surface density ( $\Gamma$ ) as a function of immersion time for ZnPQI (solid line with closed circles) and ZnPQ<sup>[20g,h]</sup> (dashed line with open circles), which adsorb on TiO<sub>2</sub> films without the scattering layer.

$1.1 \times 10^{-10} \text{ mol cm}^{-2}$ . Taking into account the good agreement between calculated and experimental  $\Gamma$  values and the saturated adsorption behavior of ZnPQI, ZnPQI forms nearly densely packed monolayers on TiO<sub>2</sub>.

Attenuated total reflectance Fourier transform infrared (ATR-FTIR) spectroscopy is a useful tool for gaining information on the binding mode of the molecules adsorbed on TiO<sub>2</sub> substrates.<sup>[19,20]</sup> The ATR-FTIR spectrum of ZnPQI obtained from a solid sample reveals the characteristic band of  $\tilde{\nu}(C=O)$  of the carboxylic acid group at around  $1700 \text{ cm}^{-1}$  (see the Supporting Information, Figure S4a),<sup>[19,20]</sup> which disappears in spectra of TiO<sub>2</sub>/ZnPQI (see the Supporting Information, Figure S4b). ATR-FTIR spectra of TiO<sub>2</sub>/ZnPQI exhibit a marked increase in the symmetric carboxylate band,  $\tilde{\nu}(COO_s^-)$ , at around  $1400 \text{ cm}^{-1}$ .<sup>[19,20]</sup> The disappearance of  $\tilde{\nu}(C=O)$  and the increased intensities of  $\tilde{\nu}(COO_s^-)$  corroborate the assumption that a proton is detached from the carboxylic acid group during adsorption of the porphyrin on the TiO<sub>2</sub> surface, leading to the bidentate binding of the carboxylate group to the TiO<sub>2</sub> surface. This is consistent with the previous assignment that a carboxylic acid of analogous porphyrins is bound to a TiO<sub>2</sub> surface through a bridging bidentate mode.<sup>[19,20,22a]</sup>

### Photovoltaic properties of porphyrin-sensitized TiO<sub>2</sub> cells

We evaluated the performance of TiO<sub>2</sub>/ZnPQI and TiO<sub>2</sub>/ZnPQ solar cells and drew comparisons between them. The TiO<sub>2</sub> electrode was sensitized with ZnPQI by immersing the TiO<sub>2</sub> electrode into the porphyrin ethanol solution for 1–8 h. The  $\eta$  value is derived from the equation:  $\eta = J_{SC} \times V_{OC} \times ff$ , where  $J_{SC}$  is the short circuit current,  $V_{OC}$  is the open circuit potential, and  $ff$  is the fill factor. The  $\eta$  value of the TiO<sub>2</sub>/ZnPQI solar cell reveals the immersion-time dependency (Figure 5), as observed in the immersion-time dependence of  $\eta$  values of TiO<sub>2</sub> solar cells sensitized with ZnPQ.<sup>[20g,h]</sup> After reaching the maximum  $\eta$  value in 2 h, the  $\eta$  value is decreased slightly with an increase in immersion time, which can be rationalized by an increase in porphyrin aggregation with increasing immersion time.<sup>[19,20,31b]</sup> The difference in immersion time for maximal  $\eta$  and  $\Gamma$  values can be explained as a trade-off between the effect of the extent of porphyrin adsorption and that of porphyrin aggregation, which would adversely affect  $\eta$  values. Notably, the  $\eta$  value of

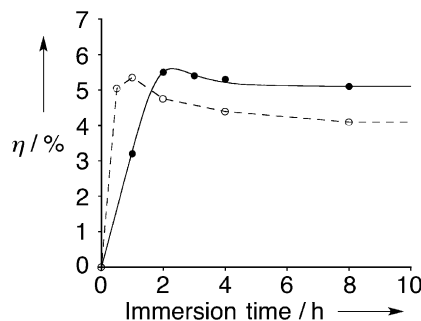


**Figure 5.** Plots of  $\eta$  as a function of immersion time for ZnPQI- (solid line with closed circles) and ZnPQ-sensitized<sup>[20g,h]</sup> (dashed line with open circles)  $\text{TiO}_2$  cells. The porphyrins were adsorbed on the  $\text{TiO}_2$  electrodes by immersing them into a solution of ZnPQI or ZnPQ (0.2 mM) in EtOH without co-adsorbent.

the ZnPQI solar cell (5.5 %) is comparable to that of the ZnPQ cell (5.4%), but the degree of decrease in the  $\eta$  value of the ZnPQI solar cell as a function of immersion time is smaller than that of the ZnPQ solar cell, probably due to the larger steric hindrance of the ZnPQI molecule.<sup>[20g,h]</sup>

To further optimize cell performance, ZnPQI (0.2 mM) was adsorbed onto the  $\text{TiO}_2$  surface for 2 h in EtOH, in which chenodeoxycholic acid (CDCA, 0.6 mM) was added as co-adsorbent to reduce porphyrin aggregation on  $\text{TiO}_2$ . Figure 6 depicts

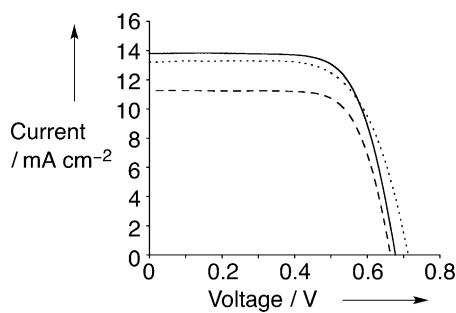


**Figure 6.** Photocurrent–voltage characteristics of the  $\text{TiO}_2/\text{ZnPQI+CDCA}$  cell (solid line;  $\eta=6.8\%$ ,  $J_{\text{SC}}=13.9 \text{ mA cm}^{-2}$ ,  $V_{\text{OC}}=0.68 \text{ V}$ ,  $ff=0.71$ ), the  $\text{TiO}_2/\text{ZnPQI}$  cell (dashed line;  $\eta=5.5\%$ ,  $J_{\text{SC}}=11.2 \text{ mA cm}^{-2}$ ,  $V_{\text{OC}}=0.67 \text{ V}$ ,  $ff=0.74$ ), and the  $\text{TiO}_2/\text{ZnPQ+CDCA}$  cell<sup>[20g,h]</sup> (dotted line;  $\eta=6.3\%$ ,  $J_{\text{SC}}=13.2 \text{ mA cm}^{-2}$ ,  $V_{\text{OC}}=0.71 \text{ V}$ ,  $ff=0.67$ ). Electrolyte: 1,3-dimethylimidazolium iodide (1.0 M),  $\text{I}_2$  (0.03 M),  $\text{LiI}$  (0.05 M), guanidinium thiocyanate (0.1 M), and 4-tert-butylpyridine (0.50 M) in acetonitrile/valeronitrile (85:15); input power: AM 1.5 under simulated solar light (100  $\text{mW cm}^{-2}$ ).

the photocurrent–voltage characteristics of  $\text{TiO}_2/\text{ZnPQI}$  and  $\text{TiO}_2/\text{ZnPQI+CDCA}$  solar cells under the respective maximal  $\eta$  conditions. Co-adsorption of CDCA had a large impact on the performance of the  $\text{TiO}_2/\text{ZnPQI+CDCA}$  cell. Under the optimized conditions the  $\text{TiO}_2/\text{ZnPQI+CDCA}$  cell exhibits:  $\eta=6.8\%$  with  $J_{\text{SC}}=13.9 \text{ mA cm}^{-2}$ ,  $V_{\text{OC}}=0.68 \text{ V}$ , and  $ff=0.71$ . It should be noted that this value is larger than that of the  $\text{TiO}_2/\text{ZnPQ+CDCA}$  cell<sup>[20g,h]</sup> under optimized conditions ( $\eta=6.3\%$ ,  $J_{\text{SC}}=13.2 \text{ mA cm}^{-2}$ ,  $V_{\text{OC}}=0.71 \text{ V}$ ,  $ff=0.67$ ). The short-circuit current and fill factor of the ZnPQI-sensitized solar cell are larger than those of the ZnPQ-sensitized solar cell, whereas the open-circuit potential of the ZnPQI-sensitized cell is smaller

than that of the ZnPQ-sensitized cell, leading to the overall improved cell performance of ZnPQI.

Photocurrent action spectra of  $\text{TiO}_2/\text{ZnPQI+CDCA}$  and  $\text{TiO}_2/\text{ZnPQ+CDCA}$  cells were also compared (Figure 7). Note that the maximal incident photon-to-current efficiency (IPCE) values

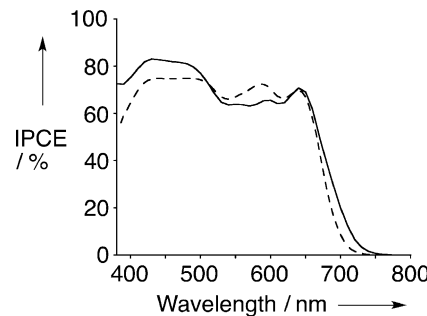


**Figure 7.** Photocurrent action spectra of the  $\text{TiO}_2/\text{ZnPQI+CDCA}$  cell (solid line) and  $\text{TiO}_2/\text{ZnPQ+CDCA}$  cell<sup>[20g,h]</sup> (dashed line).

at Soret bands are 83 % for the  $\text{TiO}_2/\text{ZnPQI+CDCA}$  cell and 75 % for the  $\text{TiO}_2/\text{ZnPQ+CDCA}$  cell.<sup>[20g,h]</sup> The photocurrent action spectra follow the absorption features of the corresponding porphyrin adsorbed on the electrodes (Figure 8),

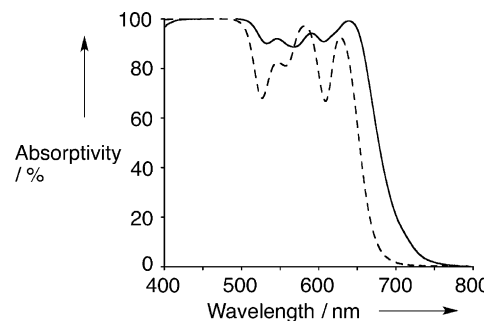


**Figure 8.** Light-harvesting efficiencies of the  $\text{TiO}_2/\text{ZnPQI+CDCA}$  (solid line) and  $\text{TiO}_2/\text{ZnPQ+CDCA}$ <sup>[20g,h]</sup> (dashed line) electrodes. The scattering  $\text{TiO}_2$  layers were not applied to  $\text{TiO}_2$  electrodes to measure absorbance accurately.

demonstrating that the porphyrin is the main source for photocurrent generation. IPCE is divided into three components according to Equation (1):

$$\text{IPCE} = \text{LHE} \times \phi_{\text{inj}} \times \eta_{\text{col}} \quad (1)$$

where LHE (light-harvesting efficiency) corresponds to the number of absorbed photons per number of incident photons,  $\phi_{\text{inj}}$  is the quantum yield for electron injection from the porphyrin excited singlet state to the CB of the  $\text{TiO}_2$  electrode, and  $\eta_{\text{col}}$  is the efficiency of charge collection. It should be noted that the  $\text{TiO}_2/\text{ZnPQI+CDCA}$  cell had superior IPCE values at wavelengths of 650–750 nm (Figure 7). Considering the effect of the light-scattering  $\text{TiO}_2$  layer, the LHE value of the  $\text{TiO}_2/\text{ZnPQI+CDCA}$  cell is larger than that of the  $\text{TiO}_2/\text{ZnPQ+CDCA}$  cell.

ZnPQ+CDCA cell, especially at 650–750 nm (Figure 8), leading to the improvement in IPCE values at 650–750 nm. Although the IPCE values of the  $\text{TiO}_2/\text{ZnPQI}+\text{CDCA}$  cell at 500–650 nm are lower than those of the  $\text{TiO}_2/\text{ZnPQ}+\text{CDCA}$  cell, the higher IPCE values of the  $\text{TiO}_2/\text{ZnPQI}+\text{CDCA}$  cell at 380–500 and 650–750 nm result in overall high  $J_{\text{SC}}$  values of the  $\text{TiO}_2/\text{ZnPQI}+\text{CDCA}$  cell relative to the  $\text{TiO}_2/\text{ZnPQ}+\text{CDCA}$  cell.

The  $V_{\text{OC}}$  value of the  $\text{TiO}_2/\text{ZnPQI}+\text{CDCA}$  cell is slightly lower than that of the  $\text{TiO}_2/\text{ZnPQ}+\text{CDCA}$  cell. To elucidate the reason for this, we measured current–voltage characteristics under dark conditions (Figure 9). The onset for the  $\text{TiO}_2/\text{ZnPQI}+\text{CDCA}$

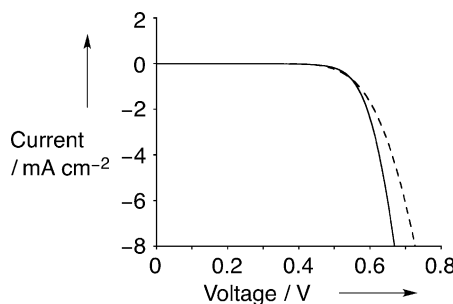


**Figure 9.** Current–voltage characteristics of the  $\text{TiO}_2/\text{ZnPQI}+\text{CDCA}$  (solid line) and the  $\text{TiO}_2/\text{ZnPQ}+\text{CDCA}$ <sup>[20g,h]</sup> (dashed line) cells under dark conditions.

cell appears at a less positive value than that of the  $\text{TiO}_2/\text{ZnPQ}+\text{CDCA}$  cell. This indicates that the degree of charge recombination between the injected electrons in the CB of  $\text{TiO}_2$  and  $\text{I}_3^-$  for the  $\text{TiO}_2/\text{ZnPQI}+\text{CDCA}$  cell is higher than that for the  $\text{TiO}_2/\text{ZnPQ}+\text{CDCA}$  cell, although the electron densities in the HOMO of ZnPQI are anticipated to be far from the  $\text{TiO}_2$  surface relative to ZnPQ obtained from DFT calculations.<sup>[35]</sup> This result can be explained plausibly by the more tilted geometry of ZnPQI relative to ZnPQ on the  $\text{TiO}_2$  surface, as we have proposed previously.<sup>[5d,31b]</sup> It should be also pointed out that longer dyes tend to be tilted on  $\text{TiO}_2$  surfaces when they are adsorbed.<sup>[31b]</sup> Given that the  $\eta_{\text{col}}$  primarily depends on the relative rates of charge transport against charge recombination, the higher charge recombination rate for the  $\text{TiO}_2/\text{ZnPQI}+\text{CDCA}$  cell relative to the  $\text{TiO}_2/\text{ZnPQ}+\text{CDCA}$  cell may also account for the feasible lower charge-collection efficiency, resulting in the slightly lower  $V_{\text{OC}}$  value.<sup>[36]</sup> At present, it is unclear why the ff value of ZnPQI-sensitized solar cells is slightly larger than that of ZnPQ-sensitized solar cells and this may stem from the relatively small cell serial resistances including electron-transport resistances in the  $\text{TiO}_2$  film.

## Conclusions

We have synthesized a push–pull porphyrin with an electron-donating triarylamino group at the  $\beta,\beta'$ -edge through the fused imidazole group and an electron-withdrawing fused carboxyquinoxalino anchoring group at the opposite  $\beta,\beta'$ -edge to address the substitution effects of the electron-donating group on the photovoltaic properties. This push–pull porphyrin

showed improved light-harvesting properties relative to the reference porphyrin. This push–pull porphyrin-sensitized solar cell exhibited a relatively high power conversion efficiency of 6.8%, which is larger than that of the reference porphyrin-sensitized solar cell (6.3%). Further improvement may be possible by introducing other electron-donating groups at the opposite side of the carboxyquinoxalino anchoring group in an effective  $\pi$ -conjugated manner and/or utilizing  $\text{Co}^{\text{II/III}}$  tris(bipyridyl)-based redox electrolytes, which are known to increase  $V_{\text{OC}}$  relative to conventional  $\text{I}^-/\text{I}_3^-$  redox electrolytes.<sup>[23h]</sup> Such fundamental information on electron-donating groups in porphyrin DSSCs will be useful for the rational molecular design of highly efficient DSSCs based on push–pull type porphyrins.

## Experimental Section

### Synthesis

ZnPQI was synthesized following the protocol developed by Crossley et al.<sup>[26]</sup> and by our group.<sup>[20g,h]</sup> Detailed synthetic routes to the target compound and the intermediates are described in the Supporting Information.

### Spectroscopy

UV/Vis absorption spectra of the porphyrins in dichloromethane and the porphyrin monolayers on  $\text{TiO}_2$  electrodes without a light-scattering layer (*vide infra*) were recorded using a Perkin–Elmer Lambda 900 UV/VIS/NIR spectrometer. Steady-state fluorescence spectra were acquired by using a SPEX Fluoromax-3 spectrofluorometer. A time-correlated single photon counting (TCSPC) method was used for the time-resolved fluorescence measurements in the nanosecond and sub-nanosecond time-scale and time resolution was approximately 60–70 ps (full width at half maximum).<sup>[29]</sup> The excitation wavelength was 405 nm and the emission decay was monitored at 658 nm. ATR-FTIR spectra were recorded with the golden gate diamond anvil ATR accessory (NICOLET 6700, Thermo Scientific), using typically 256 scans at a resolution of 2  $\text{cm}^{-1}$ . All samples were placed in contact with the diamond window using the same mechanical force.

### Electrochemistry

Electrochemical measurements were performed using an ALS 630a electrochemical analyzer. Redox potentials of the porphyrins were determined by DPV analysis in dichloromethane containing  $\text{Bu}_4\text{NPf}_6$  (0.1 M) as a supporting electrolyte. A glassy carbon working electrode (3 mm in diameter), an  $\text{Ag}/\text{AgNO}_3$  (0.01 M in acetonitrile) reference electrode, and a Pt wire counter electrode were employed. Ferrocene/ferrocenium (+0.642 V versus NHE) was used as an internal standard for all measurements. All of the measured potentials were converted to the NHE scale.

### DFT calculations

Geometry optimization and electronic structure calculations of the porphyrins were performed using the B3LYP functional and the 6-31G(d) basis set implemented in the Gaussian 03 program package.<sup>[37]</sup> Molecular orbitals were visualized by using the Molstudio 3.0 software.

## Preparation of the porphyrin-sensitized $\text{TiO}_2$ electrode and photovoltaic measurements

The preparation of  $\text{TiO}_2$  electrodes and the fabrication of sealed cells for photovoltaic measurements were performed following a previously reported method.<sup>[38]</sup> Nanocrystalline  $\text{TiO}_2$  particles ( $d=20\text{ nm}$ , CCIC:PST18NR, JGC-CCIC, and  $d=30\text{ nm}$ , CCIC:PST30NR, JGC-CCIC) were used as the transparent layer of the photoanode, whereas sub-microcrystalline  $\text{TiO}_2$  particles ( $d=400\text{ nm}$ , CCIC:PST400C, JGC-CCIC) as the light-scattering layers of the photoanode. The working electrode was prepared by cleaning a fluorine-doped tin (FTO) glass (Solar, thickness of 4 mm,  $10\text{ }\Omega/\square$ , Nippon Sheet Glass) with a detergent solution in an ultrasonic bath for 10 min, rinsing with distilled water, ethanol, and air-drying. The electrode was subjected to UV- $\text{O}_3$  irradiation for 18 min, immersed into a solution of freshly prepared aqueous  $\text{TiCl}_4$  (40 mM) at 70 °C for 30 min, washed consecutively with distilled water and ethanol, and dried. Nanocrystalline  $\text{TiO}_2$  paste was coated onto the FTO glass by screen printing, followed by standing in a clean box for a few minutes and dried at 125 °C for 6 min, and then repeating the process to attain a final thickness of 12  $\mu\text{m}$ . A layer of the sub-microcrystalline  $\text{TiO}_2$  paste (4  $\mu\text{m}$ ) was deposited in the same fashion as the nanocrystalline layer. Finally, the electrode was heated under an airflow at 325 °C for 5 min, at 375 °C for 5 min, at 450 °C for 15 min, and at 500 °C for 15 min. The thickness of the films was determined using a surface profiler (Surfcom 130A, Accretech). The size of the  $\text{TiO}_2$  film was  $0.16\text{ cm}^2$  ( $4\times 4\text{ mm}$ ). The  $\text{TiO}_2$  electrode was then subjected to immersion into a solution of freshly prepared aqueous  $\text{TiCl}_4$  (40 mM) at 70 °C for 25 min before rinsing with distilled water and ethanol, and air-drying. The electrode was sintered at 500 °C for 30 min, cooled to 70 °C, and immersed into the dye solution at 25 °C in the dark for the prescribed times. The  $\text{TiO}_2$  electrode was immersed into a solution of porphyrin in ethanol (0.20 mM). The  $\text{TiO}_2$  electrode stained with ZnPQI is denoted as  $\text{TiO}_2/\text{ZnPQI}$ . To reduce dye aggregation on  $\text{TiO}_2$ , the  $\text{TiO}_2$  electrode was also immersed into a solution of porphyrin in ethanol (0.20 mM) containing CDCA (0.60 mM) as co-adsorbent. The  $\text{TiO}_2$  electrode stained with ZnPQI and CDCA is denoted as  $\text{TiO}_2/\text{ZnPQI+CDCA}$ . The porphyrin surface coverage adsorbed on  $\text{TiO}_2$  films ( $\text{mol cm}^{-2}$ ) was determined by measuring the difference in absorbance of the  $\text{TiO}_2$  films ( $\text{TiO}_2$  area of  $1.0\text{ cm}^2$  with a thickness of 12  $\mu\text{m}$ ) without the scattering layer before and after immersion of the  $\text{TiO}_2$  film in the porphyrin solution, assuming that the molar absorption coefficient in dichloromethane is identical to that on  $\text{TiO}_2$ .

The counter electrode was prepared by drilling a small hole in a FTO glass, rinsing with distilled water and ethanol before treatment with HCl/2-propanol (0.1 M) in an ultrasonic bath for 5 min. After heating in air at 400 °C for 15 min, platinum was deposited by coating the electrode twice with a solution of  $\text{H}_2\text{PtCl}_6$  (2 mg) in ethanol (1 mL) and heating in air at 400 °C for 15 min.

The sandwich cell was prepared by using the dye-anchored  $\text{TiO}_2$  film as a working electrode and a counter Pt electrode, which were assembled with a hot-melt ionomer film of Surlyn polymer gasket (DuPont), and the superimposed electrodes were tightly held and heated at 110 °C to seal the two electrodes. The aperture of the Surlyn frame was larger than the area of the  $\text{TiO}_2$  film by 2 mm and its width was 1 mm. The hole in the counter electrode was sealed by a film of Surlyn. A hole was then made in the film of Surlyn covered on the hole by a needle. A drop of an electrolyte was put on the hole in the back of the counter electrode. It was introduced into the cell through vacuum backfilling. Finally, the hole was sealed using Surlyn film and a cover glass (thickness of 0.13–0.17 mm). The edge of the FTO outside the cell was roughened

with sandpaper. A solder was applied on each edge of the FTO electrodes. The electrolyte solution used consisted of 1,3-dimethylimidazolium iodide (1.0 M),  $\text{I}_2$  (0.03 M),  $\text{LiI}$  (0.05 M), guanidinium thiocyanate (0.1 M), and 4-*tert*-butylpyridine (0.50 M) in acetonitrile/valeonitrile (85:15).

IPCE and photocurrent–voltage ( $J-V$ ) performance were measured by means of an action-spectrum-measurement setup (CEP-2000RR, Bunkoukeiki) and a solar simulator (PEC-L10, Peccell Technologies) with a simulated sunlight of AM 1.5 (100  $\text{mW cm}^{-2}$ ), respectively: IPCE (%) =  $100 \times 1240 \times i / (W_{\text{in}} \times \lambda)$ , where  $i$  is the photocurrent density [ $\text{A cm}^{-2}$ ],  $W_{\text{in}}$  is the incident light intensity [ $\text{W cm}^{-2}$ ], and  $\lambda$  is the excitation wavelength [nm]. During the photovoltaic measurements, a black plastic mask was attached on the back of the  $\text{TiO}_2$  electrode, except for the  $\text{TiO}_2$  film region, to reduce scattering light.

## Acknowledgements

This work was supported by the Grant-in-Aids (MEXT, Japan, No. 21350100 to H.I.), the Strategic Japanese-Finnish Cooperative Program (JST), the Advanced Low Carbon Technology Research and Development Program (ALCA, JST), and the WPI Initiative (MEXT, Japan). H.H. would also wish to thank a JSPS for a fellowship for young scientists. H.S., N.T., and H.L. would like to thank the Academy of Finland for financial support.

**Keywords:** dyes/pigments • electrochemistry • porphyrinoids • sustainable chemistry • synthesis design

- [1] N. Armaroli, V. Balzani, *Angew. Chem.* **2007**, *119*, 52; *Angew. Chem. Int. Ed.* **2007**, *46*, 52.
- [2] a) B. O'Regan, M. Grätzel, *Nature* **1991**, *353*, 737; b) M. K. Nazeeruddin, A. Kay, I. Rodicio, R. Humphry-Baker, E. Müller, P. Liska, N. Vlachopoulos, M. Grätzel, *J. Am. Chem. Soc.* **1993**, *115*, 6382; c) M. Grätzel, *Acc. Chem. Res.* **2009**, *42*, 1788.
- [3] a) M. K. Nazeeruddin, F. D. Angelis, S. Fantacci, A. Selloni, G. Viscardi, P. Liska, S. Ito, T. Bessho, M. Grätzel, *J. Am. Chem. Soc.* **2005**, *127*, 16835; b) F. Gao, Y. Wang, D. Shi, J. Zhang, M. Wang, X. Jing, R. Humphry-Baker, P. Wang, S. M. Zakeeruddin, M. Grätzel, *J. Am. Chem. Soc.* **2008**, *130*, 10720; c) C.-Y. Chen, M. Wang, J.-Y. Li, N. Pootrakulchote, L. Alibabaei, C. Ngoc-le, J.-D. Decoppet, J.-H. Tsai, C. Grätzel, C.-G. Wu, S. M. Zakeeruddin, *ACS Nano* **2009**, *3*, 3103; d) Y. Chiba, A. Islam, Y. Watanabe, R. Komiya, N. Koide, L. Han, *Jpn. J. Appl. Phys.* **2006**, *45*, L638; e) L. Han, A. Islam, C. Malapaka, B. Chiranjeevi, S. Zhang, X. Yang, M. Yanagida, *Energy Environ. Sci.* **2012**, *5*, 6057.
- [4] a) A. Mishra, M. K. R. Fischer, P. Bäuerle, *Angew. Chem.* **2009**, *121*, 2510; *Angew. Chem. Int. Ed.* **2009**, *48*, 2474; b) A. Hagfeldt, G. Boschloo, L. Sun, L. Kloo, H. Pettersson, *Chem. Rev.* **2010**, *110*, 6595; c) J. N. Clifford, E. Martínez-Ferrero, A. Viterisi, E. Palomares, *Chem. Soc. Rev.* **2011**, *40*, 1635.
- [5] a) H. Imahori, T. Umeyama, S. Ito, *Acc. Chem. Res.* **2009**, *42*, 1809; b) M. V. Martínez-Díaz, G. de La Torre, T. Torres, *Chem. Commun.* **2010**, *46*, 7090; c) M. G. Walter, A. B. Rudine, C. C. Wamser, *J. Porphyrins Phthalocyanines* **2010**, *14*, 759; d) H. Imahori, T. Umeyama, K. Kurotobi, Y. Takano, *Chem. Commun.* **2012**, *48*, 4032; e) M. J. Griffith, K. Sunahara, P. Wagner, K. Wagner, G. G. Wallace, D. L. Officer, A. Furube, R. Katoh, S. Mori, A. J. Mozer, *Chem. Commun.* **2012**, *48*, 4145; f) L.-L. Lin, E. W.-G. Diau, *Chem. Soc. Rev.* **2013**, *42*, 291.
- [6] a) K. Hara, K. Sayama, Y. Ohga, A. Shinpo, S. Suga, H. Arakawa, *Chem. Commun.* **2001**, 569; b) K. Hara, M. Kurashige, Y. Danoh, C. Kasada, A. Shinpo, S. Suga, H. Arakawa, *New J. Chem.* **2003**, *27*, 783; c) Z.-S. Wang, Y. Cui, Y. Dan-oh, C. Kasada, A. Shinpo, K. Hara, *J. Phys. Chem. C* **2007**, *111*, 7224; d) Z.-S. Wang, Y. Cui, Y. Dan-oh, C. Kasada, A. Shinpo, K. Hara, *J. Phys. Chem. C* **2008**, *112*, 17011.

- [7] a) T. Horiuchi, H. Miura, S. Uchida, *Chem. Commun.* **2003**, 3036; b) T. Horiuchi, H. Miura, K. Sumioka, S. Uchida, *J. Am. Chem. Soc.* **2004**, 126, 12218; c) S. Ito, S. M. Zakeeruddin, R. Humphry-Baker, P. Liska, R. Charvet, P. Comte, M. K. Nazeeruddin, P. Péchy, M. Takata, H. Miura, S. Uchida, M. Grätzel, *Adv. Mater.* **2006**, 18, 1202; d) S. Ito, H. Miura, S. Uchida, M. Takata, K. Sumioka, P. Liska, P. Comte, P. Péchy, M. Grätzel, *Chem. Commun.* **2008**, 5194.
- [8] a) K. Hara, M. Kurashige, S. Ito, A. Shinpo, S. Suga, K. Sayama, H. Arakawa, *Chem. Commun.* **2003**, 252; b) T. Kitamura, M. Ikeda, K. Shigaki, T. Inoue, N. A. Anderson, X. Ai, T. Lian, S. Yanagida, *Chem. Mater.* **2004**, 16, 1806; c) S. Hwang, J. H. Lee, C. Park, H. Lee, C. Kim, C. Park, M.-H. Lee, W. Lee, J. Park, K. Kim, N.-G. Park, C. Kim, *Chem. Commun.* **2007**, 4887; d) C. Kim, H. Choi, S. Kim, C. Baik, K. Song, M.-S. Kang, S. O. Kang, J. Ko, *J. Org. Chem.* **2008**, 73, 7072; e) H. Im, S. Kim, C. Park, S.-H. Jang, C.-J. Kim, K. Kim, N.-G. Park, *Chem. Commun.* **2010**, 46, 1335.
- [9] a) S. Tan, J. Zhai, H. Fang, T. Jiu, J. Ge, Y. Li, L. Jiang, D. Zhu, *Chem. Eur. J.* **2005**, 11, 6272; b) W.-H. Liu, I.-C. Wu, C.-H. Lai, P.-T. Chou, Y.-T. Li, C.-L. Chen, Y.-Y. Hsu, Y. Chi, *Chem. Commun.* **2008**, 5152; c) H. Choi, C. Baik, S. O. Kang, J. Ko, M.-S. Kang, M. K. Nazeeruddin, M. Grätzel, *Angew. Chem.* **2008**, 120, 333; *Angew. Chem. Int. Ed.* **2008**, 47, 327; d) Z.-S. Wang, N. Koumura, Y. Cui, M. Takahashi, H. Sekiguchi, A. Mori, T. Kubo, A. Furube, K. Hara, *Chem. Mater.* **2008**, 20, 3993; e) G. Zhang, H. Bala, Y. Cheng, D. Shi, X. Lv, Q. Yu, P. Wang, *Chem. Commun.* **2009**, 2198; f) W. Zeng, Y. Cao, Y. Bai, Y. Wang, Y. Shi, M. Zhang, F. Wang, C. Pan, P. Wang, *Chem. Mater.* **2010**, 22, 1915; g) A. Kira, Y. Shibano, S. Kang, H. Hayashi, T. Umeyama, Y. Matano, H. Imahori, *Chem. Lett.* **2010**, 39, 448.
- [10] a) A. Ehret, L. Stuhl, M. T. Spitler, *Electrochim. Acta* **2000**, 45, 4553; b) W. Wu, J. Hua, Y. Jin, W. Zhan, H. Tian, *Photochem. Photobiol. Sci.* **2008**, 7, 63.
- [11] a) Z.-S. Wang, F.-Y. Li, C.-H. Huang, L. Wang, M. Wei, L.-P. Jin, N.-Q. Li, *J. Phys. Chem. B* **2000**, 104, 9676; b) Q.-H. Yao, L. Shan, F.-Y. Li, D.-D. Yin, C.-H. Huang, *New J. Chem.* **2003**, 27, 1277; c) Y.-S. Chen, C. Li, Z.-H. Zeng, W.-B. Wang, X.-S. Wang, B.-W. Zhang, *J. Mater. Chem.* **2005**, 15, 1654.
- [12] a) Y. Chen, Z. Zeng, C. Li, W. Wang, X. Wang, B. Zhang, *New J. Chem.* **2005**, 29, 773; b) J.-H. Yum, P. Walter, S. Huber, D. Rentsch, T. Geiger, F. Nüesch, F. De Angelis, M. Grätzel, M. K. Nazeeruddin, *J. Am. Chem. Soc.* **2007**, 129, 10320.
- [13] a) P. Y. Reddy, L. Giribabu, C. Lyness, H. J. Snaith, C. Vijaykumar, M. Chandrasekham, M. Lakshmi Kantam, J.-H. Yum, K. Kalyanasundaram, M. Grätzel, M. K. Nazeeruddin, *Angew. Chem.* **2007**, 119, 377; *Angew. Chem. Int. Ed.* **2007**, 46, 373; b) J.-J. Cid, J.-H. Yum, S.-R. Jang, M. K. Nazeeruddin, E. Martínez-Ferrero, E. Palomares, J. Ko, M. Grätzel, T. Torres, *Angew. Chem.* **2007**, 119, 8510; *Angew. Chem. Int. Ed.* **2007**, 46, 8358; c) S. Eu, T. Katoh, T. Umeyama, Y. Matano, H. Imahori, *Dalton Trans.* **2008**, 5476; d) J.-J. Cid, M. García-Iglesias, J.-M. Yum, A. Forneli, J. Albero, E. Martínez-Ferrero, P. Vázquez, M. Grätzel, M. K. Nazeeruddin, E. Palomares, T. Torres, *Chem. Eur. J.* **2009**, 15, 5130; e) S. Mori, M. Nagata, Y. Nakahata, K. Yasuta, R. Goto, M. Kimura, M. Taya, *J. Am. Chem. Soc.* **2010**, 132, 4054; f) H. Imahori, H. Iijima, T. Shimada, T. Kato, *Proc. IEEE Int. Conf. Nanotechnology* **2010**, 176; g) M. Kimura, H. Nomoto, N. Masaki, S. Mori, *Angew. Chem.* **2012**, 124, 4447; *Angew. Chem. Int. Ed.* **2012**, 51, 4371; h) M.-E. Ragoussi, J.-J. Cid, J.-H. Yum, G. de La Torre, D. Di Censo, M. Grätzel, M. K. Nazeeruddin, T. Torres, *Angew. Chem.* **2012**, 124, 4451; *Angew. Chem. Int. Ed.* **2012**, 51, 4375.
- [14] a) S. Ferrere, A. Zaban, B. A. Gregg, *J. Phys. Chem. B* **1997**, 101, 4490; b) Y. Shibano, T. Umeyama, Y. Matano, H. Imahori, *Org. Lett.* **2007**, 9, 1971; c) C. Li, J.-H. Yum, S.-J. Moon, A. Herrmann, F. Eickemeyer, N. G. Pschirer, P. Erk, J. Schöneboom, K. Müllen, M. Grätzel, M. K. Nazeeruddin, *ChemSusChem* **2008**, 1, 615; d) S. Mathew, H. Imahori, *J. Mater. Chem.* **2011**, 21, 7166.
- [15] S. Wenger, P.-A. Bpuit, Q. Chen, J. Teuscher, D. Di Censo, R. Humphry-Baker, J.-E. Moser, J. L. Delgado, N. Martín, S. M. Zakeeruddin, M. Grätzel, *J. Am. Chem. Soc.* **2010**, 132, 5164.
- [16] a) A. Kay, M. Grätzel, *J. Phys. Chem.* **1993**, 97, 6272; b) T. Ma, K. Inoue, H. Noma, K. Yao, E. Abe, *J. Photochem. Photobiol. A* **2002**, 152, 207; c) M. K. Nazeeruddin, R. Humphry-Baker, D. L. Officer, W. M. Campbell, A. K. Burnell, M. Grätzel, *Langmuir* **2004**, 20, 6514; d) L. Schmidt-Mende, W. M. Campbell, Q. Wang, K. W. Jolley, D. L. Officer, M. Nazeeruddin, M. Grätzel, *ChemPhysChem* **2005**, 6, 1253; e) A. J. Mozer, M. J. Griffith, G. Tsekouras, P. Wagner, G. G. Wallace, S. Mori, K. Sunahara, M. Miyashita, J. C. Earles, K. C. Gordon, L. Du, R. Katoh, A. Furube, D. L. Officer, *J. Am. Chem. Soc.* **2009**, 131, 15621; f) J. K. Park, H. R. Lee, J. Chen, H. Shinokubo, A. Osuka, D. Kim, *J. Phys. Chem. C* **2008**, 112, 16691; g) M. S. Kang, J. B. Oh, K. D. Seo, H. K. Kim, J. Park, K. Kim, N.-G. Park, *J. Porphyrins Phthalocyanines* **2009**, 13, 798; h) Y. Liu, N. Xiang, X. Feng, P. Shen, W. Zhou, C. Weng, B. Zhao, S. Tan, *Chem. Commun.* **2009**, 2499; i) M. Ishida, S. W. Park, D. Hwang, Y. B. Koo, J. L. Sessler, D. Y. Kim, D. Kim, *J. Phys. Chem. C* **2011**, 115, 19343; j) M. S. Kang, S. H. Kang, S. G. Kim, I. T. Choi, J. H. Ryu, M. J. Ju, D. Cho, J. Y. Lee, H. K. Kim, *Chem. Commun.* **2012**, 48, 9349.
- [17] a) S. Cherian, C. C. Wamser, *J. Phys. Chem. B* **2000**, 104, 3624; b) D. F. Watson, A. Marton, A. M. Stux, G. J. Meyer, *J. Phys. Chem. B* **2003**, 107, 10971; c) D. F. Watson, A. Marton, A. M. Stux, G. J. Meyer, *J. Phys. Chem. B* **2004**, 108, 11680; d) J. Rochford, D. Chu, A. Hagfeldt, E. Galoppini, *J. Am. Chem. Soc.* **2007**, 129, 4655; e) J. Rochford, E. Galoppini, *Langmuir* **2008**, 24, 5366; f) C. Y. Lee, J. Hupp, *Langmuir* **2010**, 26, 3760; g) C. Y. Lee, C. She, N. C. Jeong, J. T. Hupp, *Chem. Commun.* **2010**, 46, 6090.
- [18] a) G. K. Boschloo, A. Goossens, *J. Phys. Chem.* **1996**, 100, 19489; b) R. B. M. Koehorst, G. K. Boschloo, T. J. Savenije, A. Goossens, T. J. Schaafsma, *J. Phys. Chem. B* **2000**, 104, 2371; c) J. N. Clifford, G. Yahiooglu, L. R. Milgrom, J. R. Durrant, *Chem. Commun.* **2002**, 1260; d) F. Odobel, E. Blart, M. Lagrée, M. Villieras, H. Boujtita, N. El Murr, S. Caramori, C. A. Bignozzi, *J. Mater. Chem.* **2003**, 13, 502; e) J. Jasieniak, M. Johnston, E. R. Waclawik, *J. Phys. Chem. B* **2004**, 108, 12962; f) A. Forneli, M. Planells, M. A. Sarmentero, E. Martínez-Ferrero, B. C. O'Regan, P. Ballester, E. Palomares, *J. Mater. Chem.* **2008**, 18, 1652; g) J. S. Lindsey, R. W. Wagner, *J. Org. Chem.* **1989**, 54, 828; h) J. Warnan, L. Faverreau, F. Meslin, M. Severac, E. Blart, Y. Pellegrin, D. Jacquemin, F. Odobel, *ChemSusChem* **2012**, 5, 1568; i) J. M. Ball, N. K. S. Davis, J. D. Wilkinson, J. Kirkpatrick, J. Teuscher, R. Gumming, H. L. Anderson, H. J. Snaith, *RSC Adv.* **2012**, 2, 6846.
- [19] a) H. Imahori, S. Hayashi, T. Umeyama, S. Eu, A. Oguro, S. Kang, Y. Matano, T. Shishido, S. Ngamsinlapasathian, S. Yoshikawa, *Langmuir* **2006**, 22, 11405; b) A. Kira, M. Tanaka, T. Umeyama, Y. Matano, N. Yoshimoto, Y. Zhang, S. Ye, H. Lehtivuori, N. V. Tkachenko, H. Lemmettyinen, H. Imahori, *J. Phys. Chem. C* **2007**, 111, 13618; c) H. Imahori, T. Umeyama, *J. Phys. Chem. C* **2009**, 113, 9029; d) H. Imahori, S. Hayashi, H. Hayashi, A. Oguro, S. Eu, T. Umeyama, Y. Matano, *J. Phys. Chem. C* **2009**, 113, 18406.
- [20] a) S. Eu, S. Hayashi, T. Umeyama, A. Oguro, M. Kawasaki, N. Kadota, Y. Matano, H. Imahori, *J. Phys. Chem. C* **2007**, 111, 3528; b) M. Tanaka, S. Hayashi, S. Eu, T. Umeyama, Y. Matano, H. Imahori, *Chem. Commun.* **2007**, 2069; c) S. Hayashi, Y. Matsubara, S. Eu, H. Hayashi, T. Umeyama, Y. Matano, H. Imahori, *Chem. Lett.* **2008**, 37, 846; d) S. Eu, S. Hayashi, T. Umeyama, Y. Matano, Y. Araki, H. Imahori, *J. Phys. Chem. C* **2008**, 112, 4396; e) S. Hayashi, M. Tanaka, H. Hayashi, S. Eu, T. Umeyama, Y. Matano, Y. Araki, H. Imahori, *J. Phys. Chem. C **2008**, 112, 15576; f) H. Imahori, Y. Matsubara, H. Iijima, T. Umeyama, Y. Matano, S. Ito, M. Niemi, N. V. Tkachenko, H. Lemmettyinen, *J. Phys. Chem. C* **2010**, 114, 10656; g) A. Kira, Y. Matsubara, H. Iijima, T. Umeyama, Y. Matano, S. Ito, M. Niemi, N. V. Tkachenko, H. Lemmettyinen, H. Imahori, *J. Phys. Chem. C* **2010**, 114, 11293; h) H. Imahori, H. Iijima, H. Hayashi, Y. Toude, T. Umeyama, Y. Matano, S. Ito, *ChemSusChem* **2011**, 4, 797.*
- [21] a) Y. Amao, Y. Yamada, *Langmuir* **2005**, 21, 3008; b) J. R. Stromberg, A. Marton, H. L. Kee, C. Kirmaier, J. R. Diers, C. Muthiah, M. Taniguchi, J. S. Lindsey, D. F. Bocian, G. J. Meyer, D. Holten, *J. Phys. Chem. C* **2007**, 111, 15464; c) X.-F. Wang, O. Kitao, H. Zhou, H. Tamiaki, S. Sasaki, *J. Phys. Chem. C* **2009**, 113, 7954; d) X.-F. Wang, H. Tamiaki, L. Wang, N. Tamai, O. Kitao, H. Zhou, S. Sasaki, *Langmuir* **2010**, 26, 6320.
- [22] a) Q. Wang, W. N. Campbell, E. E. Bonfanti, K. W. Jolley, D. L. Officer, P. J. Walsh, K. Gordon, R. Humphry-Baker, M. K. Nazeeruddin, M. Grätzel, *J. Phys. Chem. B* **2005**, 109, 15397; b) W. M. Campbell, K. W. Jolley, P. Wagner, K. Wagner, P. J. Walsh, K. C. Gordon, L. Schmidt-Mende, M. K. Nazeeruddin, Q. Wang, M. Grätzel, D. L. Officer, *J. Phys. Chem. C* **2007**, 111, 11760.
- [23] a) C.-W. Lee, H.-P. Lu, C.-M. Lan, Y.-L. Huag, Y.-R. Liang, W.-N. Yen, Y.-C. Liu, Y.-S. Lin, E. W.-G. Diau, C.-Y. Yeh, *Chem. Eur. J.* **2009**, 15, 1403; b) H.-P. Lu, C.-L. Mai, C.-Y. Tsia, S.-J. Hsu, C.-P. Hsieh, C.-L. Chiu, C.-Y. Yeh, E. W.-G. Diau, *Phys. Chem. Chem. Phys.* **2009**, 11, 10270; c) C.-Y. Lin, Y.-C. Wang, S.-J. Hsu, C.-F. Lo, E. W.-G. Diau, *J. Phys. Chem. C* **2010**, 114, 687; d) C.-L. Mai, W.-K. Huang, H.-P. Lu, C.-W. Lee, C.-L. Chiu, Y.-R. Liang, E. W.-G. Diau, C.-Y. Yeh, *Chem. Commun.* **2010**, 46, 809; e) C.-P. Hsieh, H.-P. Lu, C.-L. Chiu, C.-W. Lee, S.-H. Chung, C.-L. Mai, W.-N. Yen, S.-J. Hsu, E. W.-G. Diau,

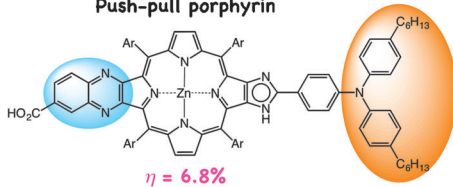
- C.-Y. Yeh, *J. Mater. Chem.* **2010**, *20*, 1127; f) S.-L. Wu, H.-P. Lu, H.-T. Yu, S.-H. Chuang, C.-L. Chiu, C.-W. Lee, E. W.-G. Diau, C.-Y. Yeh, *Energy Environ. Sci.* **2010**, *3*, 949; g) T. Bessho, S. M. Zakeeruddin, C.-Y. Yeh, E. W.-G. Diau, M. Grätzel, *Angew. Chem.* **2010**, *122*, 6796; *Angew. Chem. Int. Ed.* **2010**, *49*, 6646; h) A. Yella, H.-W. Lee, H. N. Tsao, C. Yi, A. K. Chandiran, S. M. Nazeeruddin, E. W.-G. Diau, C.-Y. Yeh, S. M. Zakeeruddin, M. Grätzel, *Science* **2011**, *334*, 629; i) Chi.-M. Lan, H.-P. Wu, T.-Y. Pan, C.-W. Chang, W.-S. Chao, C.-T. Chen, C.-L. Wang, C.-Y. Lin, E. W.-G. Diau, *Energy Environ. Sci.* **2012**, *5*, 6460; j) H.-P. Wu, Z.-W. Ou, T.-Y. Pan, C.-M. Lan, W.-K. Huang, H.-W. Lee, N. M. Reddy, Ch.-T. Chen, W.-S. Chao, C.-Y. Yeh, E. W.-G. Diau, *Energy Environ. Sci.* **2012**, *5*, 9843.
- [24] S. Bringman, S. A. Ahmed, R. Hartmann, J. Matty, *Synthesis* **2011**, *14*, 2291.
- [25] C. M. Kathryn, N. B. Konstantinos, B. Vandana, T. K. Kiran, R. B. Martin, A. F. Mark, L. V. Helen, B. D. Fernando, P. M. Andrew, *J. Org. Chem.* **2010**, *75*, 6771.
- [26] M. J. Crossley, P. J. Sintic, J. A. Hutchison, K. P. Ghiggino, *Org. Biomol. Chem.* **2005**, *3*, 852.
- [27] a) M. J. Crossley, J. A. McDonald, *J. Chem. Soc. Perkin Trans. 1* **1999**, 2429; b) D. Curiel, K. Ohkubo, J. R. Reimers, S. Fukuzumi, M. J. Crossley, *Phys. Chem. Chem. Phys.* **2007**, *9*, 5260.
- [28] F. De Angelis, S. Fantacci, A. Selloni, M. Grätzel, M. K. Nazeeruddin, *Nano Lett.* **2007**, *7*, 3189.
- [29] a) E. Maligaspe, N. V. Tkachenko, N. K. Subbaiyan, R. Chitta, M. E. Zandler, H. Lemmettyinen, F. D'Souza, *J. Phys. Chem. A* **2009**, *113*, 8478; b) N. V. Tkachenko, L. Rantala, A. Y. Tauber, J. Helaja, P. H. Hynninen, H. Lemmettyinen, *J. Am. Chem. Soc.* **1999**, *121*, 9378; c) V. Vehmanen, N. V. Tkachenko, H. Imaohori, S. Fukuzumi, H. Lemmettyinen, *Spectrochim. Acta, Part A* **2001**, *57*, 2229; d) M. Isosomppi, N. V. Tkachenko, A. Efimov, H. Lemmettyinen, *J. Phys. Chem. A* **2005**, *109*, 4881.
- [30] a) J. M. Rehm, G. L. McLendon, Y. Nagasawa, K. Yoshihara, J. Moser, M. Grätzel, *J. Phys. Chem.* **1996**, *100*, 9577; b) B. Burfeindt, T. Hannappel, W. Storck, F. Willig, *J. Phys. Chem.* **1996**, *100*, 16463; c) M. Hilgendorff, V. Sundström, *J. Phys. Chem. B* **1998**, *102*, 10505; d) J. B. Asbury, E. Hao, Y. Wang, H. N. Ghosh, T. Lian, *J. Phys. Chem. B* **2001**, *105*, 4545.
- [31] a) Y. Tachibana, S. A. Haque, I. P. Mercer, J. R. Durrant, D. R. Klug, *J. Phys. Chem. B* **2000**, *104*, 1198; b) H. Imaohori, S. Kang, H. Hayashi, M. Haruta, H. Kurata, S. Isoda, S. E. Canton, Y. Infahsaeng, A. Kathiravan, T. Pascher, P. Chábera, A. P. Yartsev, V. Sundström, *J. Phys. Chem. A* **2011**, *115*, 3679.
- [32] J. B. Foresman, A. Frisch in *Exploring Chemistry with Electronic Structure Methods*, Gaussian Inc., Pittsburgh, **1995**.
- [33] B. Liu, W. Zhu, Y. Wang, W. Wu, X. Li, B. Chen, Y.-T. Long, Y. Xie, *J. Mater. Chem.* **2012**, *22*, 7434.
- [34] D. P. Hagberg, T. Edvinsson, T. Marinado, G. Boschloo, A. Hagfeldt, L. Sun, *Chem. Commun.* **2006**, 2245.
- [35] We attempted the introduction of an  $\text{Al}_2\text{O}_3$  blocking layer to the  $\text{TiO}_2$  surface to inhibit charge recombination. The  $V_{OC}$  value was slightly increased ( $\approx 50$  mV) by the introduction, but the  $J_{SC}$  value was drastically decreased, resulting in the low  $\eta$  value (4.3%).
- [36] a) K. Hara, K. Miyamoto, Y. Abe, M. Yanagida, *J. Phys. Chem. B* **2005**, *109*, 23776; b) R. Chen, X. Yang, H. Tian, X. Wang, A. Hagfeldt, L. Sun, *Chem. Mater.* **2007**, *19*, 4007.
- [37] a) J. S. Binkley, J. A. Pople, W. J. Hehre, *J. Am. Chem. Soc.* **1980**, *102*, 939; b) Gaussian 03, M. J. Frisch, G. W. Trucks, H. B. Schlegel, G. E. Scuseria, M. A. Robb, J. R. Cheeseman, J. A. Montgomery, Jr., T. Vreven, K. N. Kudin, J. C. Burant, J. M. Millam, S. S. Iyengar, J. Tomasi, V. Barone, B. Mennucci, M. Cossi, G. Scalmani, N. Rega, G. A. Petersson, H. Nakatsuji, M. Hada, M. Ehara, K. Toyota, R. Fukuda, J. Hasegawa, M. Ishida, T. Nakajima, Y. Honda, O. Kitao, H. Nakai, M. Klene, X. Li, J. E. Knox, H. P. Hratchian, J. B. Cross, V. Bakken, C. Adamo, J. Jaramillo, R. Gomperts, R. E. Stratmann, O. Yazyev, A. J. Austin, R. Cammi, C. Pomelli, J. W. Ochterski, P. Y. Ayala, K. Morokuma, G. A. Voth, P. Salvador, J. J. Dannenberg, V. G. Zakrzewski, S. Dapprich, A. D. Daniels, M. C. Strain, O. Farkas, D. K. Malick, A. D. Rabuck, K. Raghavachari, J. B. Foresman, J. V. Ortiz, Q. Cui, A. G. Baboul, S. Clifford, J. Cioslowski, B. B. Stefanov, G. Liu, A. Liashenko, P. Piskorz, I. Komaromi, R. L. Martin, D. J. Fox, T. Keith, M. A. Al-Laham, C. Y. Peng, A. Nanayakkara, M. Challacombe, P. M. W. Gill, B. Johnson, W. Chen, M. W. Wong, C. Gonzalez, J. A. Pople, Gaussian, Inc., Wallingford, CT, **2004**.
- [38] S. Ito, T. Murakami, P. Comte, P. Liska, C. Grätzel, M. K. Nazeeruddin, M. Grätzel, *Thin Solid Films* **2008**, *516*, 4613.

Received: November 14, 2012

Published online on ■■■, 0000

## FULL PAPERS

Push-pull porphyrin



**Pushing and pulling:** A push–pull porphyrin with an electron-donating and an electron-withdrawing group at opposite sites has been synthesized to evaluate the effect of the push–pull structure

on optical, electrochemical, and photo-voltaic properties. This system exhibited a power conversion efficiency that is higher than that of the dye without the electron-donating group.

H. Hayashi, A. S. Touchy, Y. Kinjo,  
K. Kurotobi, Y. Toude, S. Ito, H. Saarenpää,  
N. V. Tkachenko, H. Lemmetyinen,  
H. Imahori\*



Triarylamine-Substituted Imidazole-  
and Quinoxaline-Fused Push-Pull  
Porphyrins for Dye-Sensitized Solar  
Cells

